2019-03-01

Mathematical modelling of microtubule-tau protein transients: insights into the superior mechanical behavior of axon

Li, Long-yuan

10.1016/j.apm.2019.02.030
Applied Mathematical Modelling
Elsevier

To be published in "Applied Mathematical Modelling"
Received 11 October 2017, Revised 17 February 2019, Accepted 25 February 2019
https://doi.org/10.1016/j.apm.2019.02.030

Mathematical modelling of microtubule-tau protein transients: insights into the superior mechanical behavior of axon

Jiayu Wu[a,b], Hong Yuan[a,*], Long-yuan Li[b], Bing Li[c], Kunjie Fan[b], Shanqing Li[a], Kin-Nam Lee[d]

[a]MOE Key Laboratory of Disaster Forecast and Control in Engineering, Institute of Applied Mechanics, Jinan University, Guangzhou 510632, China

[b]School of Engineering, University of Plymouth, Plymouth PL4 8AA, UK

[c]Blackett Laboratory, Imperial College London, South Kensington Campus, SW7 2AZ, UK

[d]Medway School of Pharmacy, University of Kent, Chatham ME4 4TB, UK

* Corresponding author: Hong Yuan, E-mail: tyuanhong@jnu.edu.cn

ABSTRACT

Axons with staggered microtubules cross-linked by tau protein possess a remarkable mechanical balance of high specific stiffness and toughness. Owing to their viscoelastic nature, axons exhibit stress rate-dependent mechanical behavior, which is relevant to their selective vulnerability to damage in traumatic brain injury. A Kelvin-Voigt viscoelastic shear lag model is developed to elucidate the mechanical responses of axons under transient tensile force. Analytical closed-form expressions are derived to characterize the relative sliding, stress transfer and failure mechanism between microtubule and tau protein while the axon is stretched transiently. The results from the theoretical solutions elucidate how the MT-tau interface length and stress rate affect the mechanical responses of axon. It is found that axonal failure mechanism may be different under different loading conditions. Long microtubules are more vulnerable to rupture at high stress rate, yet short microtubules are likely to detach from microtubule bundles under large deformations. In the view of multi-level failure of axon, it is illustrated how the vulnerable axons protect themselves from overall damage, and how the axon can simultaneously achieve an outstanding mechanical balance of high specific stiffness and toughness.

KEYWORDS: Staggered composite; Biocomposite; Shear lag model; Kelvin-Voigt viscoelastic model; Traumatic brain injury

1. Introduction

Staggered biocomposites are found to exhibit a remarkable mechanical balance of fracture toughness *versus* stiffness and strength [1, 2]. In consideration of the structure of staggered biocomposite and the vulnerability of axon, it may possess the innate ability of mechanical balance of high stiffness and high toughness, and self-protecting over the course of evolution; hence the axon is taken as an example for investigation in this study.

Traumatic brain injury (TBI) is primarily resulted from an impact to the brain tissue from an external mechanical force including contact force, penetration of a projectile, or inertia forces induced by rapid

acceleration and deceleration [3]. In recent years, TBI has become a major public health issue, killing 15 per 100,000 individuals in European countries [4] and affecting over 2.5 million people in the USA [5] per year.

Plenty of *in vitro* researches indicated that the mechanical rupture of microtubules (MTs) results in traumatic brain injury, commonly referred to as "concussion" [6, 7]. As depicted in Fig. 1a, a single long slender axon and multiple shorter dendrites are responsible for transmitting and receiving signals, respectively [8]. Histologically, axonal cytoskeleton consists of MT bundles connected by microtubule-associated protein (MAP) tau, as illustrated in Fig. 1b [8, 9]. Parallel array of MTs, acting as reinforcing components with a main function of transporting electrochemical cargo, are the stiffest structural element within the axon [10-13].

Owing to their viscoelastic nature, axons exhibit strain or stress rate-dependent rupture [7]. In order to characterize the micromechanical breaking of axonal ultrastructure, axons were uniaxially stretched transiently by using transmission electron microscopy (TEM) under different strain rates [6, 7]. Experimental techniques are tricky to capture the immediate mechanical behavior of axonal MT bundles in tension. It is reported that the axon behaved like an elastic element while it is subjected to sudden changes in force [14]. Indeed, viscoelasticity may be more appropriate to capture the major biophysical behavior of axon and associated MTs in such conditions.

In recent years, there is an increasing interest in modelling the mechanical response of axon. However, little is known about which component of the axonal cytoskeleton might break under transient mechanical loading and large deformation. Tolomeo et al. [15] reported that cross-linking proteins provided shear resistance between MTs. Peter et al. [16] used a discrete bead-spring model to simulate the biomechanical behavior of axonal microtubule bundle under uniaxial tension, and they assumed that both MT and tau protein are linear elastic materials. Shamloo et al. [17] considered MTs as a large number of discrete masses and modelled tau protein as Kelvin-Voigt element so that viscoelastic model can be employed to simulate the transient response of axonal MTs under sudden forces. de Rooij et al. modelled the time-dependent behaviour of brain tissue by adopting an analytical hyperelastic approach [18], and developed a computational mechanics model to elucidate cellular-level characteristics of MT bundles [19]. Combined with experimental results and finite element analysis (FEA), viscosity has been identified as the most critical factor causing the mechanical vulnerability of axon under transient loading [10].

Within the axonal cytoskeleton, tau protein plays a vital role in the assembly of individual MTs [20], and the breaking of tau protein may be relevant to some of neurodegenerative diseases, such as Alzheimer's disease [21, 22] and Parkinsonism [23]. Different viscoelastic models consisting of linear elastic MT and viscoelastic tau protein, a combination of elastic springs and viscous dashpots, were postulated to elucidate the macroscopic viscoelastic behavior of the axon by some researchers [14, 24, 25]. Ahmadzadeh et al. [10] verified that Kelvin viscoelastic model can efficiently characterize the viscoelastic mechanical behavior of axon, but only MT failure is investigated in their model without consideration of tau protein breaking. However, once tau protein axial strain exceeds its ultimate strain, MTs will detach from the MT bundle [26, 27]. What's more, tau protein breaking is found to be associated with some of neurodegenerative diseases. Therefore, it's significant to develop a

computational model comprehensively characterizing the axonal failure evidence of MT rupture and tau protein breaking.

Though many researches revealed the mechanical behavior of tau protein and MTs [10, 14, 24, 25], the molecular mechanism of axonal failure remains poorly understood. In Ref. [28] we have investigated MT-tau interface failure mechanism under transient torsional loading. Our goals of this study is to start a dialog between experimentalists and modelers, so that experimentalists are more informed about what type of data is needed for model development and validation. At the microscopic length scale of axon, randomly staggered alignment of discontinuous MTs are held together by connective tau proteins. The objective of this work is to investigate the mechanical response of axons under transient tensile force and the fundamental design principles of biocomposites for engineering fiber reinforce composites. To explore the mechanical responses of axons, shear lag model (SLM) including viscoelastic tau proteins is developed to predict the relative sliding and stress transfer in the axon under transient loading. In order to accomplish these research objectives, three research questions are to be answered:

1. The structure of vulnerable axon is mainly composed of parallel staggered reinforcing MTs cross-linked by tau protein. What kind of superior mechanical properties does the axon have?
2. How does the vulnerable axon protect itself from overall damage over the course of evolution?
3. How does the axon simultaneously achieve an outstanding mechanical balance of high specific stiffness and toughness?

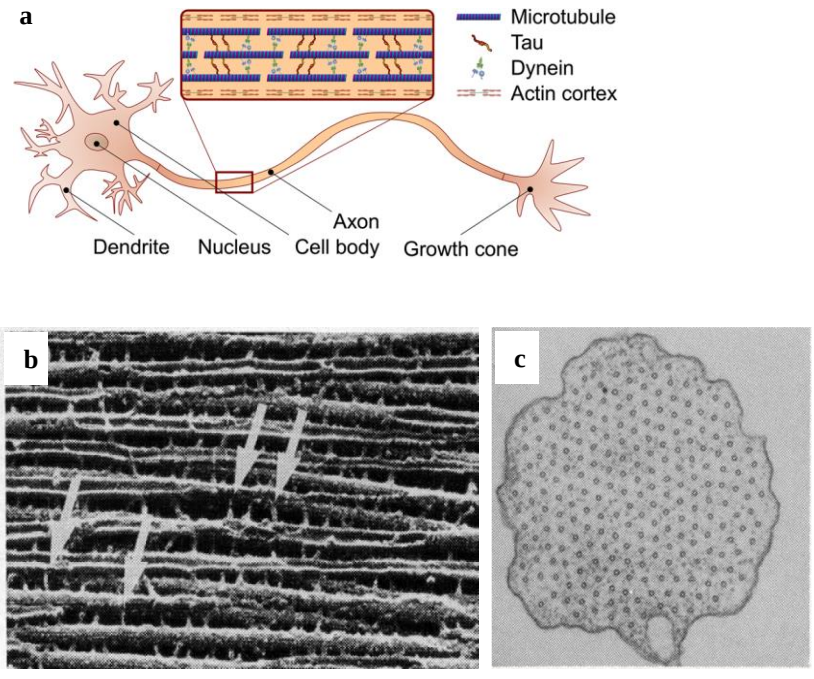

Fig. 1. (a) Neuron and cross-section diagram of the axon, reprinted from [19]; (b) Electron microscopy image of axonal MTs cross-linked by tau proteins (Arrows); (c) Cross-sectional electron micrograph of MT bundle, adapted from [29].

2. Materials and methods

2.1. Fundamental formulas and theoretical derivation

In 1952, SLM was firstly proposed by Cox [30], which has now been modified and developed for biomechanical applications [31-38]. SLM can be employed to characterize stress transfer between MTs and tau protein under transient tensile conditions. As shown in Fig. 2a, the cytoskeleton of MT is hollow cylindrical structures with outer radius R_O and inner radius R_I. As the elastic modulus of MTs is much larger than that of tau protein, MTs are assumed to follow linear elastic constitutive relation, and its Young's modulus is denoted by E_M.

Before theoretical derivations, the assumptions are adopted in the analysis presented in this study as follows:

(i) The stiffest discontinuous MTs are connected by tau protein, leading to deformation and deformation rate primarily occur in tau protein, thus, all the MTs are assumed to be linear elastic materials, and tau protein follows viscoelastic constitutive law.

(ii) The MT-tau interface length L is over two orders of magnitude larger than the distance between adjacent MTs so that the deformation in axon is essentially along x-direction.

(iii) All the MTs are parallel array along x-direction, and the MT-tau interface length L is nearly half of their entire length (see Fig. 2a).

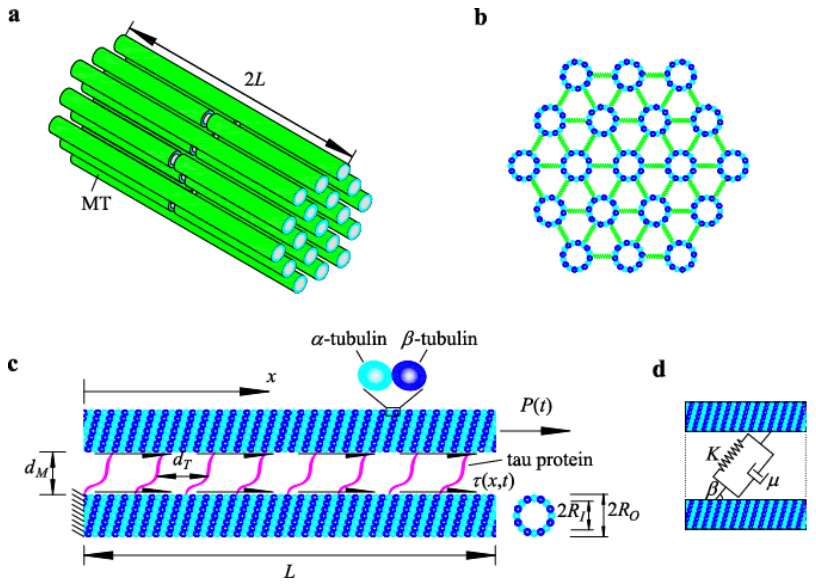

Fig. 2. (a) The microstructure of the axon. (b) Cross-sectional image of hexagonal MT bundle connected by tau proteins. (c) Unit cell used in viscoelastic SLM. (d) SLM containing Kelvin-Voigt viscoelastic tau protein.

Recently, researchers found that axons have viscoelastic material behavior [5, 17, 39, 40]. Based on the experiment [41], a Kelvin-Voigt viscoelastic model containing a spring with stiffness K in parallel with a dashpot with viscosity μ (Fig. 2d) is employed for tau protein in order to predict the biomechanical behavior of axon subjected to transient tensile force

$$\eta\dot{\delta}+\delta=\frac{F}{K} \tag{1}$$

where $\eta=\mu/K$ is tau protein dashpot timescale. A Cartesian coordinate system is established at the midpoint of an entire length of MT so that the longitudinal direction of MTs is along x-axis (see Fig.

2c). In the existing study of axon [10], the axon is simplified as a staggered arrangement of discontinuous MTs connected by tau proteins, which is represented by a periodic unit cell that is half the entire length of MT. When the unit cell is stretched by a tensile force, stress will be transferred from one MT to the adjacent MTs through tau protein, which leads to relative sliding between MTs. Tau protein elongation δ and the relative sliding between adjacent MTs $[u_1(x,t)–u_2(x,t)]$ follow the geometrical relationship as follows

$$\delta(x,t) \approx \left[u_1(x,t) - u_2(x,t)\right]\cos\beta \tag{2}$$

where β is the angle between the tau protein and the MT; u_1 and u_2 are displacements of upper and lower MTs, respectively.

Tensile forces $F(x,t)$ resulting from the elongation of tau protein can be converted to shear stress $\tau(x,t)$ acting over the entire MT circumference, which can be written as

$$\tau(x,t) = \frac{\alpha F(x,t)\cos\beta}{2\pi R_O d_T} \tag{3}$$

where d_T is the center-to-center distance between neighboring tau protein. The number of adjacent MTs is α=6 based on the cross-sectional electron micrograph of MT bundle (Fig. 1c and Fig. 2b).

According to the unit cell (see Fig. 2c) showing the two adjacent MTs, shear stress $\tau(x,t)$ acts over the MT circumference leading to the following equilibrium equations

$$\frac{\partial \sigma_1(x,t)}{\partial x} = \frac{2R_O}{R_O^2 - R_I^2}\tau(x,t) \tag{4}$$

$$-\frac{\partial \sigma_2(x,t)}{\partial x} = \frac{2R_O}{R_O^2 - R_I^2}\tau(x,t) \tag{5}$$

where R_O and R_I are the outer radius and inner radius of the MTs, respectively. σ_1 and σ_2 are the normal stresses of the linear elastic upper and lower MTs, which can be expressed as

$$\sigma_1(x,t) = E_M\varepsilon_1 = E_M\frac{\partial u_1(x,t)}{\partial x},\quad \sigma_2(x,t) = E_M\varepsilon_2 = E_M\frac{\partial u_2(x,t)}{\partial x} \tag{6}$$

where E_M is the Young's modulus of MTs. ε_1 and ε_2 are the axial strain of the upper and lower MTs, respectively.

While MT has a negligible mass, at any point x along MTs longitude direction, the tensile force $P(t)$ should maintain mechanical balance with the normal stresses acting on the MT cross-section, thus we can obtain

$$\sigma_1(x,t)S + \sigma_2(x,t)S = P(t) \tag{7}$$

where $S=\pi(R_O^2-R_I^2)$ is the cross-sectional area of MT.

Letting

$$\zeta^2 = \eta,\quad L_C^2 = \frac{E_M d_T S}{2\alpha K\cos^2\beta} \tag{8}$$

and combining Eqs. (1)-(8), we can get the governing equation for tau protein elongation

$$\frac{\partial\delta}{\partial t} = \frac{L_C^2}{\zeta^2}\frac{\partial^2\delta}{\partial x^2} - \frac{1}{\zeta^2}\delta \tag{9}$$

The upper MT normal stress σ_1 along the x-direction can be written as

$$\sigma_1 = \frac{E_M}{2\cos\beta}\frac{\partial\delta}{\partial x} + \frac{P}{2S} \tag{10}$$

with boundary conditions $\sigma_1(0,t)=0$, $\sigma_1(L,t)=P(t)/\pi(R_O^2-R_I^2)$. Based on Eq. (10), boundary and initial conditions are alternatively expressed as

$$\frac{\partial\delta(0,t)}{\partial x} = -\frac{P(t)\cos\beta}{E_M S}, \quad \frac{\partial\delta(L,t)}{\partial x} = \frac{P(t)\cos\beta}{E_M S} \tag{11}$$

$$\delta(x,0) = \varphi(x) \tag{12}$$

where L_C is the characteristic length over which the stress is transferred between MT and tau protein.

Tau protein elongation can be derived from solving the nonhomogeneous partial differential equation (Eq. (9)) with nonhomogeneous boundary conditions (Eq. (11)) and initial condition (Eq. (12))

$$\delta(x,t) = \left[C_0 + D_0(t)\right]e^{-\frac{1}{\zeta^2}t} + \sum_{n=1}^{\infty}\left[C_n + D_n(t)\right]e^{-\left(\frac{1}{\zeta^2}+\frac{L_C^2}{\zeta^2}\frac{n^2\pi^2}{L^2}\right)t}\cos\frac{n\pi x}{L} + \frac{P(t)\cos\beta}{E_M S}\left(\frac{x^2}{L}-x\right) \tag{13}$$

where

$$C_0 = \frac{1}{L}\int_0^L\left[\varphi(x) - \frac{P(0)\cos\beta}{E_M SL}x^2 + \frac{P(0)\cos\beta}{E_M S}x\right]dx$$

$$C_n = \frac{2}{L}\int_0^L\left[\varphi(x) - \frac{P(0)\cos\beta}{E_M SL}x^2 + \frac{P(0)\cos\beta}{E_M S}x\right]\cos\frac{n\pi x}{L}dx$$

$$D_0(t) = \int_0^t e^{\frac{1}{\zeta^2}s}h_0(s)ds$$

$$D_n(t) = \int_0^t e^{\left(\frac{L_C^2}{\zeta^2}\frac{n^2\pi^2}{L^2}+\frac{1}{\zeta^2}\right)s}h_n(s)ds$$

$$h_0(t) = \frac{1}{L}\int_0^L H(x,t)dx$$

$$h_n(t) = \frac{2}{L}\int_0^L H(x,t)\cos\frac{n\pi x}{L}dx$$

$$H(x,t) = \frac{\cos\beta}{\zeta^2 E_M SL}\left[2L_C^2P(t) - P(t)x^2 + P(t)Lx - \zeta^2P'(t)x^2 + \zeta^2P'(t)Lx\right]$$

It can be seen from the above equations that, the values of C_0 and C_n depend on the initial condition. If there are no elongation and no force in the beginning, we can get $C_0=C_n=0$. D_0 and D_n are determined by the force $P(t)$ stretched at the midpoint of the entire MT.

After the expression of tau protein elongation is gained, the solutions for normal stress in the MT and shear stress acting over the MT circumference yield

$$\sigma_1(x,t) = \sigma_2(x-L,t) = -\frac{n\pi}{2L}\sum_{n=1}^{\infty}\left[C_n + D_n(t)\right]e^{-\left(\frac{1}{\zeta^2}+\frac{L_C^2}{\zeta^2}\frac{n^2\pi^2}{L^2}\right)t}\sin\frac{n\pi x}{L} + \frac{2P(t)\cos\beta}{SL}x - \frac{P(t)\cos\beta}{2S} \tag{14}$$

$$\tau(x,t) = -\frac{n^2\pi^2\left(R_O^2-R_I^2\right)}{4R_O L^2}\sum_{n=1}^{\infty}\left[C_n + D_n(t)\right]e^{-\left(\frac{1}{\zeta^2}+\frac{L_C^2}{\zeta^2}\frac{n^2\pi^2}{L^2}\right)t}\cos\frac{n\pi x}{L} + \frac{P(t)\cos\beta}{SL} \tag{15}$$

Obviously, MT axial strain can be derived from Eq. (6). Tau protein axial strain can be derived from the definition of axial strain $\varepsilon_T=\delta\sin\beta/d_M$, where d_M is the surface-to-surface distance between adjacent

MTs.

2.2. Failure criteria and universal applicability of the solutions

In general, the mechanical properties of strength and toughness are mutually exclusive [42]; yet these properties are a significant requirement for most structural materials. Strength is invariably a stress representing a material's resistance to non-recoverable deformation [43]. When the transient tensile force continuously exerts at the end of the MT, the main component of either MT or tau protein will reach the ultimate strain. It was reported that MTs are shown to be ruptured under 50% of axial strain by several researchers [44-46]. With increasing strain, tau-tau bonds begin to break in exceed of approximately 40% [41].

Once MT axial strain reaches 50%, MT ruptures and transient loading comes to an end. Detachment of MT from bundle occurs at x=0 and x=L once tau protein axial strain reaches >40%. Thus, three typical types of axonal failure may appear when MTs are increasingly stretched by a transient tensile force, as shown in Fig. 3. Fig. 3 records the axonal failure during the time (upper: MT sliding; left: MT rupture; middle: a portion of MT detachment; right: MT rupture; bottom: all the MT detachment). Generally, breaking of the bonds between the paired tau proteins starts from both ends and propagates sequentially toward the midpoint of the MT-tau interface. L_s and L_d denote the MTs sliding length and detachment length, respectively (see Fig. 3). Solutions in sliding region (Eqs. (13)-(15)) remain valid in case a) the initiation of tau protein elongation at both ends is considered as the initial condition $\varphi(x)$; b) the Cartesian coordinate system moves the right with the distance of L_d; c) L is replaced by L_s. As MTs are assumed to be linear elastic material, solutions in MTs detachment region can be easily obtained.

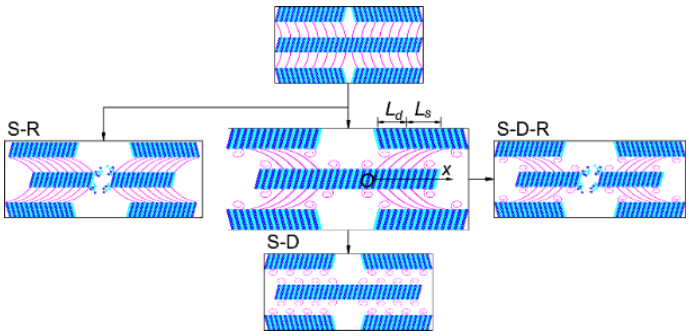

Fig. 3. Three types of axonal failure. (a) MT rupture with no breaking of tau-tau bonds, namely sliding-rupture (S-R) regime; (b) The detachment of MTs with all the tau-tau bond failure, namely sliding-detachment (S-D) regime; (c) Parts of tau-tau bond breaking before MT rupture, namely sliding-detachment-rupture (S-D-R) regime.

2.3. Related experiments and parameters

It can be noted from Eq. (9) that, the micromechanical interaction behavior of axon is determined by $(L_C/\zeta)^2$ and $1/\zeta^2$. These two parameters depends on the geometrical and material parameters of MT and tau protein, excluding the MT-tau interface length L. Nevertheless, boundary and initial conditions are determined by external force $P(t)$ and the MT-tau interface length L. In brief, the mechanical response of axon bundle depends on external force and geometrical and material properties of MT and tau

protein.

Experimental data from numerous researches are applied to assign values to the parameters in viscoelastic SLM [9, 16, 17, 41, 44-49]. The length of MT is about 1-10 μm, and its outer and inner diameters are 25 nm and 14 nm, respectively [9]. Axonal MTs are hexagonally aligned with surface-to-surface spacing of approximately 20 nm [16, 17, 29]. In general, the Young's modulus of MT could be captured by the slope of its stress-strain curve. The ultimate tensile strain of MT can be defined as the axial strain when the MT ruptures. The Young's modulus of MTs was found to be 1.51 ± 0.19 GPa [9], which agreed well with experimental data reported by Suresh [50]. The rupture tensile strain can be set at 50% according to experimental measurements of the MT rupture strain performed by Janmey et al. [44], consistent with Suresh's experimental observation [50].

The geometrical and material parameters of tau protein are also of great significance. About 95% of tau proteins are formed by paired helical filaments with a radius of 4-10 nm [47]. Based on statistical analysis, Hirokawa et al. [48] reported that tau protein center-to-center spacing fell within the typical range, 20-40 nm. The Young's modulus of tau protein is typically about 5 MPa [16, 49], which gives the tau cross-link axial spring constant of 33.3 pN/nm as calculated from $K=E_T\pi R_T^2\sin\beta/d_M$. According to the experimental data [41], Ahmadzadeh et al. [10] estimated the viscoelastic parameter η=0.35 s by using Bell's equation [51]. Additionally, interactions in hTau40 broke at maximum force 300 pN observed by Wegmann et al. [41], and therefore tau protein breaking tensile strain is estimated in exceed of 40%.

In the current work, the geometrical and material parameters are gained originally from experiment data or estimations, as listed in Table 1. The angle β between the tau protein and the MT is assumed to be 60°. According to these parameters, we can obtain the characteristic length from Eq. (8), L_C=0.390 μm.

Table 1 Variables and values for viscoelastic SLM

Variable	Value	References
R_O	12.5 nm	[9]
R_I	7 nm	[9]
R_T	4-10 nm	[47]
E_M	1.5 GPa	[49]
d_M	20-38 nm	[20]
d_T	20-40 nm	[48]
$2L$	1-10 μm	[9]
K	33.3 pN/nm	[16, 49]
η	0.35 s	[10, 41]
-	50%	[44-46]
-	40%	[41]

3. Results

3.1. Analysis of axonal failure process

3.1.1. Prediction of the axon failure mode

Axonal MTs are experimentally found to be parallel arrays, with an average length of 4 μm [3]. Fig. 4 shows the maximum MT and tau protein axial strain history of MT-tau interface length about 2 μm. It can be noted from Fig. 4 that MT and tau protein reach their ultimate strain at the same time when $\dot{\sigma}$ =92.5E_M Pa/s, which indicates that MT failure and tau protein failure occur simultaneously at applied stress rate $\dot{\sigma}$ =92.5E_M Pa/s. When the applied stress rate is 100E_M Pa/s, MT reaches its ultimate strain firstly, thus axonal failure follows the S-R regime. Otherwise, it follows either S-D regime or S-D-R regime. Additionally, axon failure process under different stress rates is illustrated in Fig. 4b.

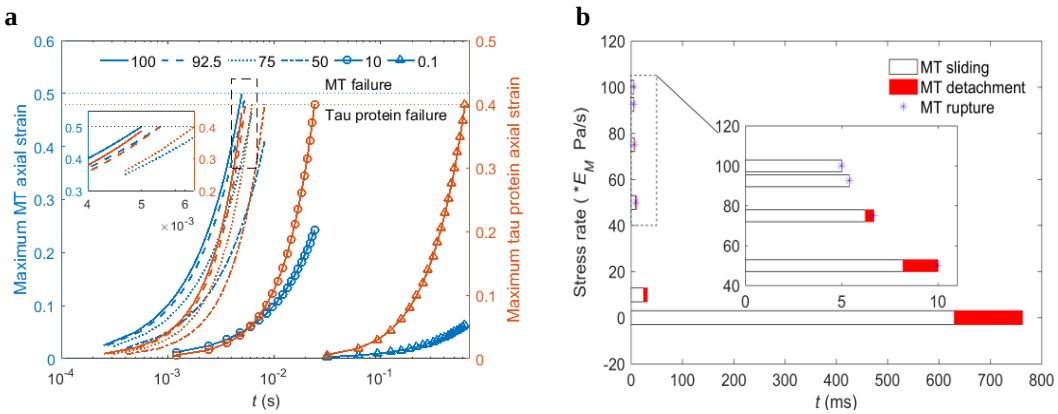

Fig. 4. (a) Prediction of the time sequence of MT failure and tau protein failure. The blue and orange lines capture the maximum MT and tau protein axial strains, respectively; and different linetypes characterize different stress rates. (b) Axon failure process under different stress rates. Model parameter used in calculation are n=1-30, R_O=12.5 nm, R_I=7 nm, E_M=1.5 GPa, R_T=7 nm, d_M=20 nm, d_T=30 nm, β=60°, α=6, K=33.3 pN/nm, η=0.35 s, L=5L_C=1.9479 μm, stress rate $\dot{\sigma}$ =100E_M, 92.5E_M 75E_M, 50E_M, 10E_M, 0.1E_M Pa/s.

3.1.2. Sliding-rupture regime

Fig. 5 shows the maximum axial strain of tau protein at both ends of the MT-tau interface length (L), and the minimum tau protein axial strain at the center, which agrees with the analytical results [17]. The maximum and minimum axial strains of MTs are found to be at the midpoint and both ends of the entire MT length (2L), respectively. Under the applied stress rate $\dot{\sigma}$ =92.5E_M Pa/s, the initiation breaking of tau-tau bond and MT rupture occur at the same time; yet MTs come to failure first at the applied stress rate $\dot{\sigma}$ =100E_M Pa/s, and MT-tau interface remains intact at all times. While MT is continuously stretched at a high stress rate, tau protein axial strain is extremely large at both ends (x=0 or L), but is nearly zero in the region 0.1<x/L<0.9 (Fig. 5a and 5c). The axial strain distribution of the upper MT and lower MT surrounding the midpoint (0.1<x/L<0.9) remain constant, which equals to half of the maximum strain (Fig. 5b and 5d). It can be noted from Fig. 5b and 5d that, evidence of MT

rupture is more sensitive to stress rate rather than tensile stress, consistent with the experimental observation in the region of axonal swelling by Tang-Schomer et al. [7]. MTs are considered as the tracks for chemical cargo transport, and they will rupture under high stress rate ($\dot{\sigma} \geq 92.5E_M$ Pa/s) found in TBI, leading to the transport interruption [6, 7]. This mathematical modelling can help us to understand the mechanism of TBI, and predict the symptom appearance of TBI when the brain is subjected to sudden external mechanical forces.

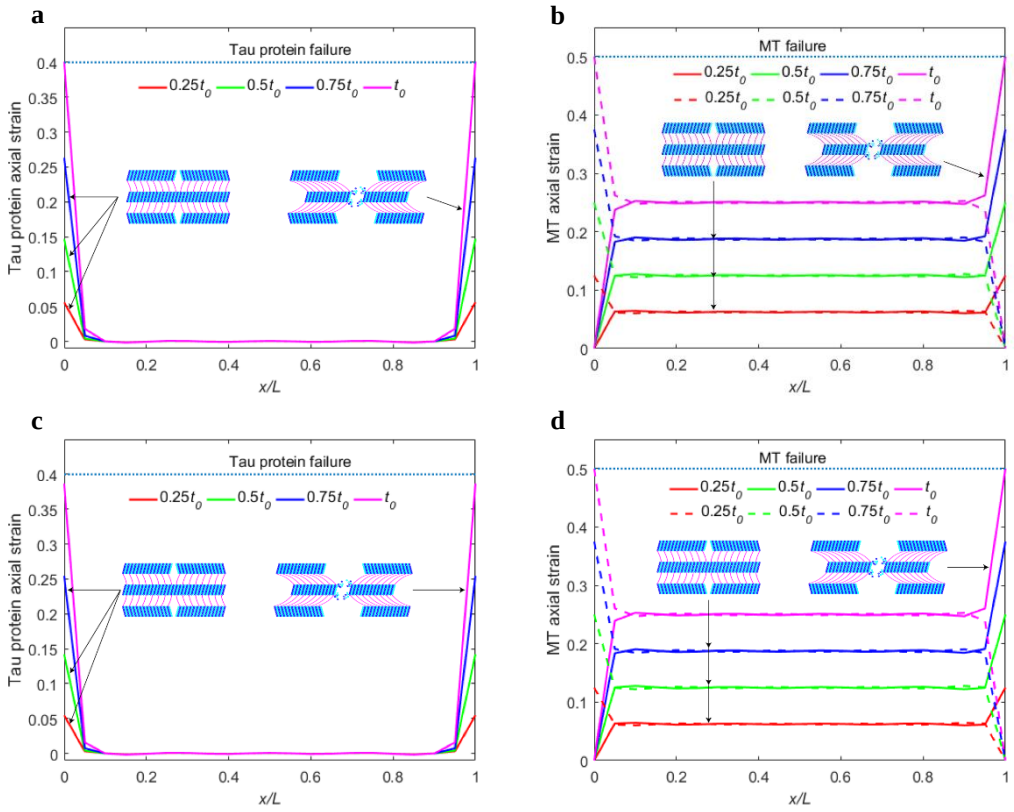

Fig. 5. Distribution of (a) tau protein axial strain along the MTs and (b) MT axial strain with $L=5L_C=1.9479$ μm, stress rate $\dot{\sigma}=92.5E_M$ Pa/s, MT rupture time $t_0=0.0054$ s; (c) tau protein axial strain along the MTs and (d) MT axial strain with $L=5L_C=1.9479$ μm, stress rate $\dot{\sigma}=100E_M$ Pa/s, MT rupture time $t_0=0.005$ s (In Fig. 5b and 5d, solid line and dashed line represent the upper MT and the lower MT plotted in Fig. 2c, respectively).

3.1.3. Sliding-detachment regime

The second type of axonal failure is caused by tau protein breaking, leading to MT detachment from MT bundle. Tau protein and MT axial strain are shown in Fig. 6. When applied stress rate are much smaller than $92.5E_M$ Pa/s, e.g. $\dot{\sigma}=10E_M$ Pa/s or $0.1E_M$ Pa/s, axonal failure follows S-D regime. It can be seen from Fig. 6 that, as the stretched loading continuously increases, the breaking of bonds between the paired tau proteins starts from both ends and propagates sequentially toward the midpoint of the MT-tau interface, as observed in the experiment [16]. According to the MT detachment time, MT-tau interface breaks faster and faster, as the applied loading increases continuously.

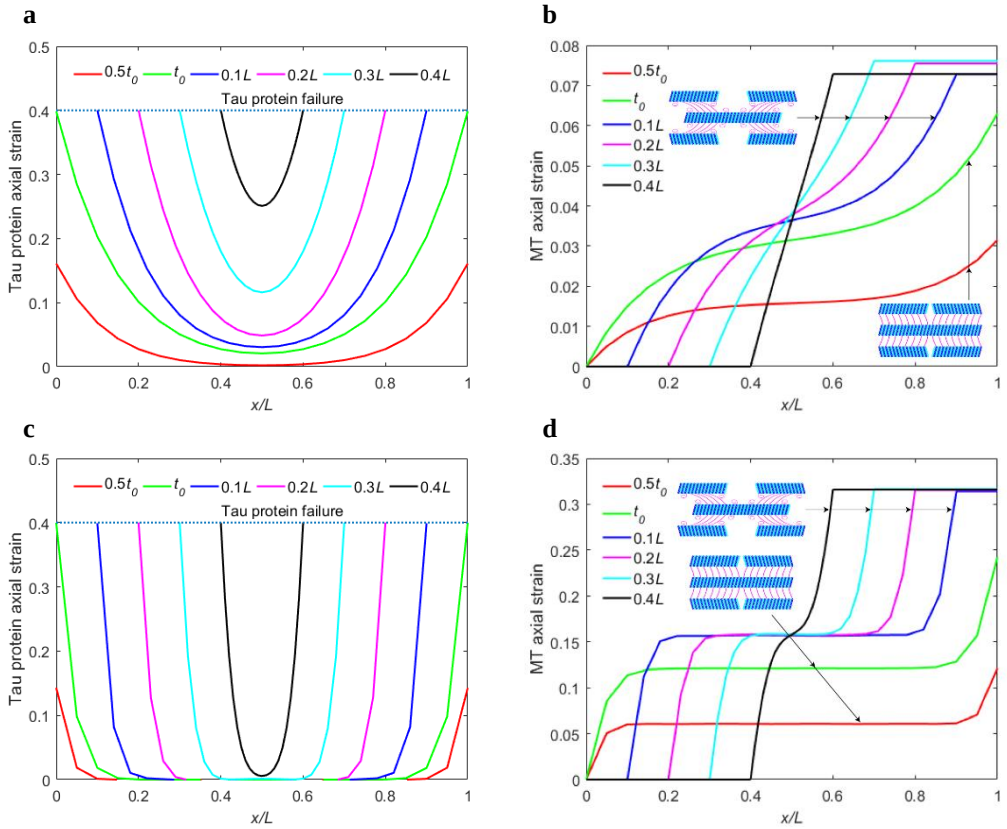

Fig. 6. Distribution of (a) tau protein axial strain along the MTs and (b) MT axial strain with L=5L_C=1.9479 μm, stress rate $\dot{\sigma}$ =0.1E_M Pa/s, tau-tau bonds breaking time t_0=0.6298 s, MTs detachment length 0.1L, 0.2L, 0.3L, 0.4L occurs at 0.7280 s, 0.7552 s, 0.7615 s, 0.7623 s; (c) tau protein axial strain along the MTs and (d) MT axial strain with L=5L_C=1.9479 μm, stress rate $\dot{\sigma}$ =10E_M Pa/s, tau-tau bonds breaking time t_0=24.22 ms, MTs detachment length 0.1L, 0.2L, 0.3L and 0.4L occurs at 31.4061 ms, 31.5396 ms, 31.5926 ms and 31.6083 ms. Axial strain of the lower MT can be obtained from symmetry condition, thus it is not provided herein.

3.1.4. Sliding-detachment-rupture regime

A complicated failure process of axon, containing tau protein breaking and MT rupture, is illustrated in Fig. 7. When applied stress rate is slightly smaller than 92.5E_M Pa/s, e.g. $\dot{\sigma}$ =50E_M Pa/s or 75E_M Pa/s, shear stress will be concentrated at both ends of the MT-tau interface even though the relative sliding is small. Obviously, tau protein closed to both ends breaks first, and then MTs rupture not until all the connected tau proteins come to failure, as shown in Fig. 7.

Both MT rupture and tau protein breaking will occur in different MT-tau interface lengths under transient loading conditions [3, 16]. However, to the best of our knowledge, there is no experimentally

reported data characterizing this complicated type of axonal failure—a portion of MT detachment and MT rupture successively happen to the same MT, although this type of axonal failure may happen in the light of our theoretical prediction, which is different from the S-R axonal failure regime.

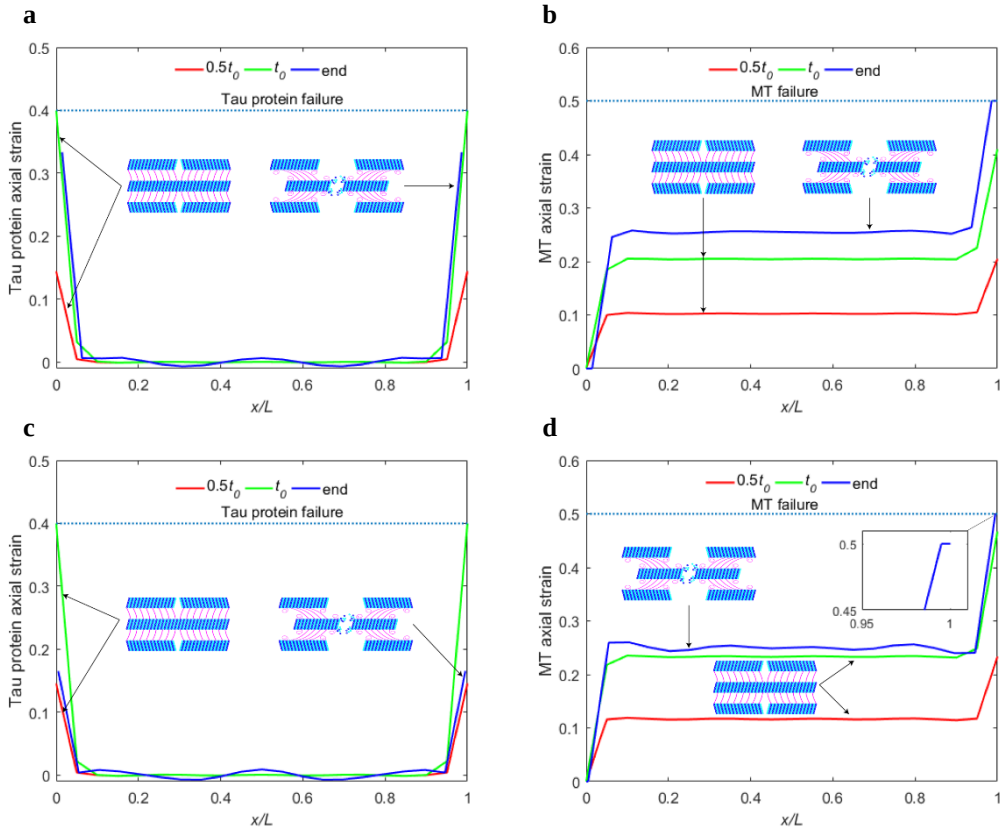

Fig. 7. Distribution of (a) tau protein axial strain along the MTs and (b) MT axial strain with L=5L_C=1.9479 μm, stress rate $\dot{\sigma}$ =50E_M Pa/s, tau-tau bonds breaking time t_0=8.1893 ms, MT rupture time (end) at 10 ms; (c) tau protein axial strain along the MTs and (d) MT axial strain with L=5L_C=1.9479 μm, stress rate $\dot{\sigma}$ =75E_M Pa/s, tau-tau bonds breaking time t_0=6.222 ms, MT rupture time (end) at 6.667 ms.

3.2. Effect of the stress rate on axonal failure process

In this section, we investigate the strain distribution at different stress rates by comparing Figs. 5-7. While axon is stretched under $\dot{\sigma}$ >50E_M Pa/s, axial strain of tau protein at both ends (x=0 and L) is extremely large and tau protein axial strain in the region 0.1<x/L<0.9 is close to zero; the MT axial strain distribution surrounding the midpoint (x=L/2) remains constant. While the applied stress rate is very small, the tau protein axial strain distribution surrounding the midpoint (x=L/2) is not close to zero, and MT axial strain surrounding the midpoint is variable, as shown in Fig. 6a. Thus, we can conclude that during the loading process MT axial strain along the interface length is nearly unchanged, and tau-tau bonds break simultaneously in the end if the applied stress rate is small enough (quasi-static).

In order to clarify the relationship between the applied stress rate and mechanical response of axons containing Kelvin-Voigt viscoelastic tau protein, the time and spatial coordinate system should be rescaled as $T=\dot{\sigma}t$, $X=x/L$, in such a way that variables in Eq. (9) are normalized as $\Delta(X,T)=\delta/L$, $\partial\Delta/\partial T=(\partial\delta/\partial t)/(\dot{\sigma}L)$, $\partial^2\Delta/\partial X^2=(\partial^2\delta/\partial x^2)/L$. According to the rescale variables, Eq. (9) can be converted to

$$\frac{\dot{\sigma}\mu}{K}\frac{\partial\Delta}{\partial T}=\frac{L_C^2}{L^2}\frac{\partial^2\Delta}{\partial X^2}-\Delta \tag{16}$$

Eq. (16) implies that tau protein with high viscosity has similar relative sliding with high applied stress rate when all other parameters remain the same. On the contrary, tau protein with high spring constant has an opposite tendency. Interestingly, axon bundle can withstand strains of over 100% and recover to its original configuration without evidence of damage [7]. However, axons appeared to failure when subjected to a sudden change in tensile force [52]. Yuen et al. [53] reported that MT rupture begins at axon strain 5%, when axon is stretched under strain rate 50 s^{-1}. This viscoelastic shear lag model can explain why the axonal injury is sensitive to the stress rate.

3.3. Effect of the MT-tau interface length on stress transfer

Researchers found that the interface length affects the stress transferring and fracture propagation between fiber and matrix in the composites and biocomposites [54, 55]. Recently, finite element models were established to explore how MT-tau interface length affects the mechanical behavior of axon [10]. In this study, SLM including viscoelastic tau protein is constructed in order to illustrate the effects of MT-tau interface length on relative sliding and stress transfer under transient tensile force, as shown in Fig. 8.

While MTs are stretched by a force with a low stress rate $\dot{\sigma}$ =0.001E_M Pa/s, tau protein axial strain along short MT-tau interface length (L=L_C) is very large (Fig. 8c). Whereas if the applied stress rate is 10E_M Pa/s, tau protein axial strains in both ends are identical, which indicates that the initiation of tau protein breaking starts simultaneously, and overall tau proteins along the short interface length come to failure in a shorter period of time (Fig. 8a). Normal stress in the MT will be concentrated at the both ends when the stress rate is high and MT-tau interface is long enough, as illustrated in Fig. 8b and 8d.

Histologically, long and short MTs are parallel aligned in the axon bundle. Bass et al. [56] found that different lengths of MT have different mechanical functions. Long MT is responsible for carrying loads, which results in a higher resistance to the sliding [57], and implies that long MTs are more susceptible to rupture. Yet, tau proteins in the short MT-tau interface are responsible for sliding, which may explain the significant elongation of axon following traumatic stretch. Our model prediction is consistent with the experimental observation proposed by Peter et al. [16].

a **b**

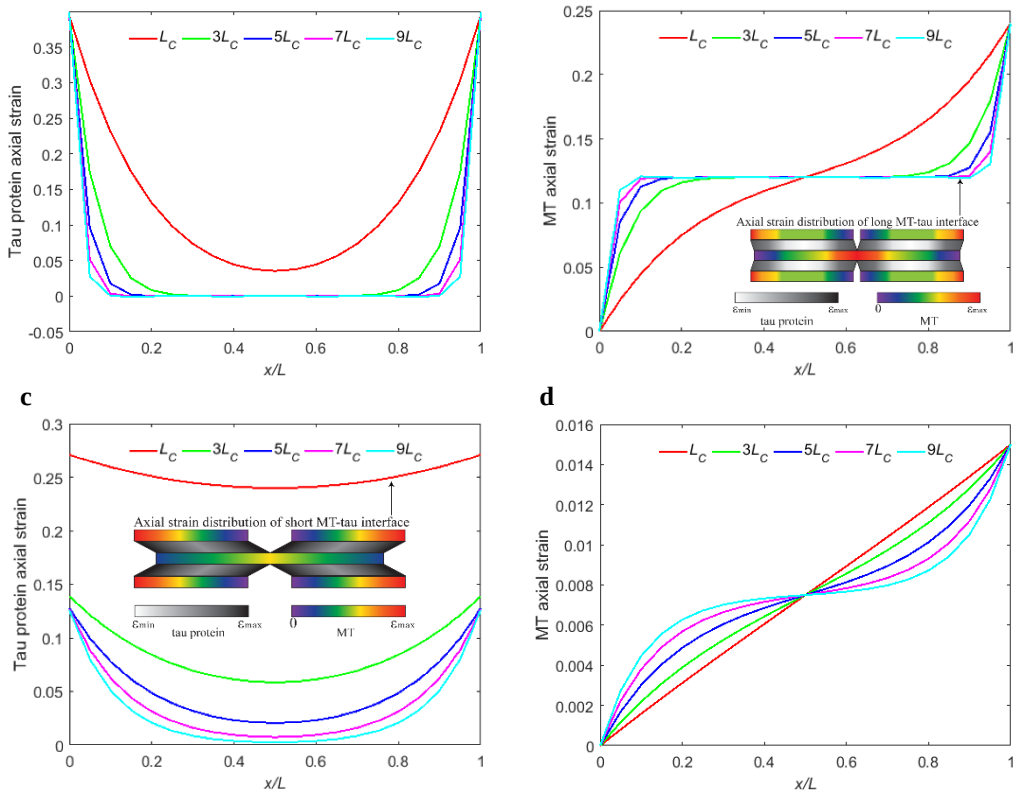

Fig. 8. Distribution of (a) tau protein axial strain along the MTs and (b) MT axial strain under stress rate $\dot{\sigma}$ =10E_M Pa/s, at the time t=0.024 s; (c) tau protein axial strain along the MTs and (d) MT axial strain under stress rate $\dot{\sigma}$ =0.001E_M Pa/s, at the time t=30 s.

3.4. Effective stiffness of axon

Micromechanical analysis can provide a basis for the mechanical performance of macrostructures. For instance, the Young's modulus of axon bundle could be computed from the ratio of the average force over the MT cross-sectional area and the average strain $u_1(L,t)/L$:

$$E(t)=\frac{c_M L\sigma_1(L,t)}{2u_1(L,t)} \tag{17}$$

where c_M is MT volume fraction. For the hexagonal lattice of MTs, c_M can be expressed as

$$c_M=\frac{\pi\left(R_O^2-R_I^2\right)}{\left(d_M+2R_O\right)^2\sin 60^\circ} \tag{18}$$

A mathematical model has been established to characterize the mechanical properties of axon at a nano-scale, where MTs and tau proteins act as coupled Kelvin-Voigt viscoelastic systems. Scientists have powerful experimental equipment, such as TEM, atomic force microscopy (AFM) and microelectromechanical systems (MEMS), etc., but it's difficult to measure the elongation of tau protein along the MTs and axial strain of MTs. A general discussion on the stress-strain or force-displacement relation of axon, obtained from the experiments, can be found in Refs. [14, 58].

A series of *in vivo* tensile tests on axon were recently conducted to measure the mechanical properties

of axon [14, 59-61]. Impressively, Rajagopalan et al. [14] reported that the axons behave like elastic springs under suddenly applied force condition. The effective stiffness of the axons, represented by the slope of the force-deformation curve, takes values in the range 0.2-1.2 nN/μm. The force-deformation curve of axonal bundle under tensile stress is plotted in Fig. 9. It shows that the slope of force-elongation curve of our current model agrees well with that of experimental data, which implies that our prediction for the effective stiffness of the axonal bundles is in excellent agreement with the existing experiment.

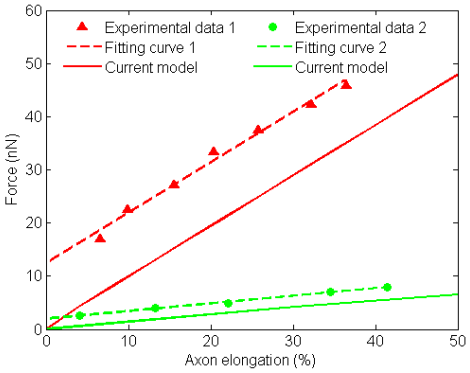

Fig. 9. Force-deformation curves of two axons from different *Drosophila* neurons. The triangles and circles represent experimental data measured by Rajagopalan et al. [14]. The dashed lines are fitting by experimental data. Our models are calculated with the parameter E_M=1.5 GPa, d_T=20 nm (red solid-line) and E_M=1.0 GPa, d_T=40 nm (green solid-line).

4. Discussion

Diffuse axonal injury (DAI) is one of the most common types of TBI [53]. Unfortunately, today's imaging methods are unable to detect the microscopic diffuse injuries to the axon [62-64]. Moreover, tension of axon bundle is such a tricky experiment, which has been prompting scientists to resort to computational modelling. Computational modelling is considered as an efficient tool to predict the mechanical response of axons for substantially improving contemporary understanding of the underlying pathology and molecular mechanisms of axonal injury.

From the perspective of material mechanics, the stiffest structural component MTs reinforce the axon, guaranteeing high stiffness of axon. Additionally, weakest-linking tau proteins ensure large deformation of the axon. The stiffest discontinuous MTs are weakest-linked by tau protein, making vulnerable axon can withstand large deformation and tensile force, achieving high stiffness and toughness. Under low stress and low stress rate conditions, axons are highly compliant and ductile, and MTs slide smoothly. Long MTs in the axon break with all tau proteins binding at high stress rate ($\dot{\sigma} \geq 92.5E_M$ Pa/s). When the applied stress rate is low ($\dot{\sigma} \leq 10E_M$ Pa/s), tau proteins along short MT-tau interface are more likely to break, and short MTs will detach from the MT bundle in the end. Under slightly high stress rate ($10E_M$ Pa/s$< \dot{\sigma} <92.5E_M$ Pa/s), parts of the tau proteins located at the both ends of slightly long MTs break at first, and then MTs come to failure. In other words, MAP tau will sacrifice themselves to protect MTs from overall damage when $\dot{\sigma} <92.5E_M$ Pa/s, and *vice versa* when it is under suddenly

applied forces condition ($\dot{\sigma} \geq 92.5E_M$ Pa/s). The type of axonal mechanical failure is multi-level, as illustrated in Fig. 10. Therefore, the vulnerable axon can achieve high stiffness and toughness, protecting itself from overall damage.

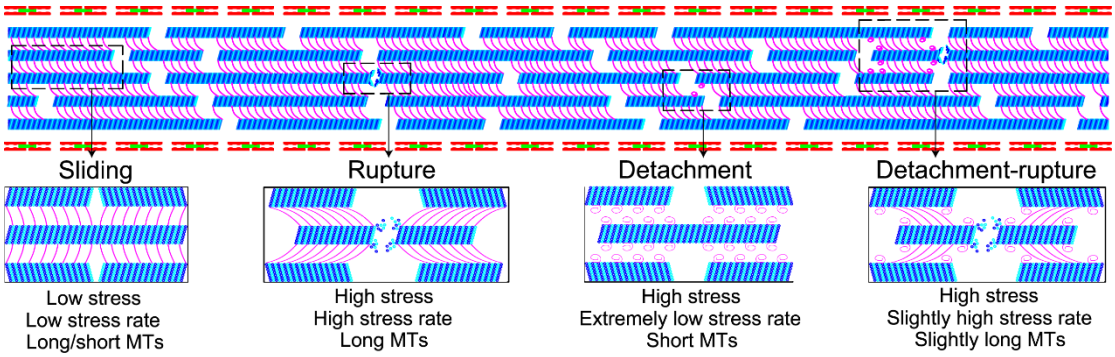

Fig. 10. Different types of deformation and damage evolution in the axon after TBI due to various MT-tau interface lengths and stress rates. Tau protein serves as a molecular switch between MT sliding, rupture, detachment and detachment-rupture.

In our previous study [65], we have explained that the fundamental load-carrying elements of regularly staggered biocomposite structures are discontinuous fibers, instead of continuous long fibers along the entire tissue. The discontinuous fibers are more capable to protect themselves from overall damage. As for axons, MTs and tau proteins will come to failure at different locations in the axon bundle, rather than break in a single section, and therefore an overall mechanical stability and high toughness could be achieved. This may be a key reason why randomly staggered biocomposite structures are observed in the axon.

The mechanical properties of engineering fiber reinforced composites depend to a great extent on the bond length. In contrast to the axon, high-performance fiber reinforced composites typically use continuous fibers, thus achieving high stiffness and strength but presenting limited toughness and ductility. From the above analysis, we know that the use of discontinuous fibers could potentially improve the ductility and fracture toughness [66, 67]. Longer interface length is not conducive to stress transfer, but discontinuous fibers could help dissipate energy and protect biocomposites from overall damage. Additionally, crack bridging by discontinuous fibers can make brittle materials tougher by transferring stress from the crack tip to the ductile matrix.

Despite the ultrastructure of the axon has the advantage of dissipating energy, MTs are vulnerable to rupture at high stress rate ($\dot{\sigma} \geq 92.5E_M$ Pa/s), resulting in TBI. The rupture of MTs results in accumulation of transported cargo in axonal swellings [7]. Fortunately, MT has the ability to recover to its original configuration through self-repair [13, 68]. In addition, TBI may trigger chronic traumatic encephalopathy. Progressive axonal injury and structural degradation are considered as the classical features of chronic traumatic encephalopathy. These symptoms may be related to Parkinsonism and Alzheimer's disease [23, 28, 69].

From the perspective of biomedical engineering, this viscoelastic SLM is likely to become the core of the broader multi-scale model in time and space. As for the time, the computational window from

milliseconds to years can explain axonal injuries in the gradual deterioration of the mechanism of time. This can help identify the early markers of neurodegenerative disease and promote early treatment. As for the space, bridging from MTs to MAP tau can explain the molecular mechanism within the axon, which can provide new coping strategies to slow, block or reverse neurodegenerative disease [70]. This viscoelastic SLM may be a crucial step for shedding new light on the complicated interactions in MT-tau transient.

Though the viscoelastic SLM provides a new method to predict the axonal injuries under comparatively high stress rate over a typical timescale from microseconds to decades of seconds, the current study is not without limitations. A major limitation of this work is the choice of the Kelvin-Voigt model, which cannot represent stress relaxation. Surely if the axon is deformed and held at the final deformation, stress relaxation occurs in the tau protein. In order to accurately predict the underlying pathophysiology of DAI, future work will seek to improve the accuracy of the model by relaxing some assumptions and considering more of the related biomedical phenomena.

5. Conclusions

The aim of this study is to explore how the axon can simultaneously achieve a remarkable mechanical balance of high specific stiffness and toughness, and why the randomly staggered alignment microtubules are selected in the axon. Of course, viscosity is one of the significant physical attributes for axons [6, 7], which will cause them to be sensitive to loading speed. In this study, we have extended the previous SLM by including Kelvin-Voigt viscoelastic behaviors for the tau protein of the axon subjected to transient loading. This Kelvin-Voigt viscoelastic SLM is an essential extension to the previous SLM which only considered the elastic or elasto-plastic behaviors under static or quasi-static conditions. Kelvin-Voigt viscoelastic SLM has been developed to elucidate the biomechanical behavior between microtubules and tau protein in the axon under transient loading. Theoretical closed-form solutions is presented to predict the stress transfer and failure forms while axon is stretched transiently. According to the recent experiments [14, 60] and results presented in this paper, the conclusions can be drawn as follows:

(1) The maximum axial strain of tau protein is at both ends of the MT-tau interface length, and the minimum tau protein axial strain is at the center. The maximum and minimum axial strains of MTs are at the midpoint and both ends of the entire MT length, respectively.

(2) Axonal failure mechanism may be different under different loading conditions, such as microtubule rupture, detachment and detachment-rupture. In the process of MT-tau protein interface failure, tau protein serves as a molecular switch. Long microtubules are more vulnerable to rupture at high stress rate, yet short microtubules are likely to detach from the microtubule bundle under large deformations.

(3) Discontinuous, stiffest and randomly staggered alignment microtubules weakest-linked by tau proteins enable axon to withstand large deformations and have the advantage of dissipating energy. In this case, the forms of axonal mechanical failure is multi-level resulting in protecting the axon from overall damage. Therefore, composites with randomly staggered element can simultaneously achieve an outstanding mechanical balance of high strength and high toughness.

Acknowledgements

The authors gratefully acknowledge the financial support provided by the National Natural Science Foundation of China (No. 11032005) and Academician Workstation of Guizhou Province Department of Science and Technology (No. (2015) 4004). The first author would like to acknowledge the financial support received from China-UK PhD placement programme (Newton Fund PhD programme by British Council and China Scholarship Council) for his study at Plymouth Marine Laboratory. Also, the authors are grateful to the anonymous reviewers for their insightful comments which have helped to improve the quality of the paper.

References

[1] Naleway SE, Porter MM, McKittrick J, Meyers MA. Structural design elements in biological materials: application to bioinspiration. Advanced Materials. 2015;27:5455-76.

[2] Espinosa HD, Filleter T, Naraghi M. Multiscale Experimental Mechanics of Hierarchical Carbon‐Based Materials. Advanced Materials. 2012;24:2805-23.

[3] Lazarus C, Soheilypour M, Mofrad MR. Torsional behavior of axonal microtubule bundles. Biophysical journal. 2015;109:231-9.

[4] Tagliaferri F, Compagnone C, Korsic M, Servadei F, Kraus J. A systematic review of brain injury epidemiology in Europe. Acta neurochirurgica. 2006;148:255-68.

[5] Hay J, Johnson VE, Smith DH, Stewart W. Chronic traumatic encephalopathy: the neuropathological legacy of traumatic brain injury. Annual Review of Pathology: Mechanisms of Disease. 2016;11:21-45.

[6] Tang-Schomer MD, Johnson VE, Baas PW, Stewart W, Smith DH. Partial interruption of axonal transport due to microtubule breakage accounts for the formation of periodic varicosities after traumatic axonal injury. Experimental neurology. 2012;233:364-72.

[7] Tang-Schomer MD, Patel AR, Baas PW, Smith DH. Mechanical breaking of microtubules in axons during dynamic stretch injury underlies delayed elasticity, microtubule disassembly, and axon degeneration. The FASEB Journal. 2010;24:1401-10.

[8] Conde C, Cáceres A. Microtubule assembly, organization and dynamics in axons and dendrites. Nature Reviews Neuroscience. 2009;10:319-32.

[9] Pampaloni F, Lattanzi G, Jonáš A, Surrey T, Frey E, Florin E-L. Thermal fluctuations of grafted microtubules provide evidence of a length-dependent persistence length. Proceedings of the National Academy of Sciences. 2006;103:10248-53.

[10] Ahmadzadeh H, Smith DH, Shenoy VB. Viscoelasticity of tau proteins leads to strain rate-dependent breaking of microtubules during axonal stretch injury: predictions from a mathematical model. Biophysical journal. 2014;106:1123-33.

[11] Goldstein LS, Yang Z. Microtubule-based transport systems in neurons: the roles of kinesins and dyneins. Annual review of neuroscience. 2000;23:39-71.

[12] Lu W, Gelfand VI. Moonlighting Motors: Kinesin, Dynein, and Cell Polarity. Trends in Cell Biology. 2017.

[13] Schaedel L, John K, Gaillard J, Nachury MV, Blanchoin L, Théry M. Microtubules self-repair in

response to mechanical stress. Nature materials. 2015;14:1156-63.
[14] Rajagopalan J, Tofangchi A, Saif MTA. Drosophila neurons actively regulate axonal tension in vivo. Biophysical journal. 2010;99:3208-15.
[15] Tolomeo J, Holley M. Mechanics of microtubule bundles in pillar cells from the inner ear. Biophysical journal. 1997;73:2241-7.
[16] Peter SJ, Mofrad MR. Computational modeling of axonal microtubule bundles under tension. Biophysical journal. 2012;102:749-57.
[17] Shamloo A, Manuchehrfar F, Rafii-Tabar H. A viscoelastic model for axonal microtubule rupture. Journal of biomechanics. 2015;48:1241-7.
[18] de Rooij R, Kuhl E. Constitutive modeling of brain tissue: current perspectives. Applied Mechanics Reviews. 2016;68:010801.
[19] de Rooij R, Miller K, Kuhl E. Modeling molecular mechanisms in the axon. Computational Mechanics. 2016:1-15.
[20] Rosenberg KJ, Ross JL, Feinstein HE, Feinstein SC, Israelachvili J. Complementary dimerization of microtubule-associated tau protein: Implications for microtubule bundling and tau-mediated pathogenesis. Proceedings of the National Academy of Sciences. 2008;105:7445-50.
[21] Ballatore C, Lee VM-Y, Trojanowski JQ. Tau-mediated neurodegeneration in Alzheimer's disease and related disorders. Nature Reviews Neuroscience. 2007;8:663-72.
[22] Spires-Jones TL, Stoothoff WH, de Calignon A, Jones PB, Hyman BT. Tau pathophysiology in neurodegeneration: a tangled issue. Trends in neurosciences. 2009;32:150-9.
[23] van den Bedem H, Kuhl E. Tau-ism: the Yin and Yang of microtubule sliding, detachment, and rupture. Biophysical journal. 2015;109:2215.
[24] Dennerll TJ, Lamoureux P, Buxbaum RE, Heidemann SR. The cytomechanics of axonal elongation and retraction. The Journal of cell biology. 1989;109:3073-83.
[25] Jérusalem A, García-Grajales JA, Merchán-Pérez A, Peña JM. A computational model coupling mechanics and electrophysiology in spinal cord injury. Biomechanics and modeling in mechanobiology. 2014;13:883-96.
[26] Ackbarow T, Chen X, Keten S, Buehler MJ. Hierarchies, multiple energy barriers, and robustness govern the fracture mechanics of α-helical and β-sheet protein domains. Proceedings of the National Academy of Sciences. 2007;104:16410-5.
[27] Ackbarow T, Keten S, Buehler MJ. A multi-timescale strength model of alpha-helical protein domains. Journal of Physics: Condensed Matter. 2008;21:035111.
[28] Wu JY, Yuan H, Li LY. Mathematical modelling of axonal microtubule bundles under dynamic torsion. Applied Mathematics and Mechanics. 2018;39:829-44.
[29] Chen J, Kanai Y, Cowan N, Hirokawa N. Projection domains of MAP2 and tau determine spacings between microtubules in dendrites and axons. Nature. 1992;360:674.
[30] Cox H. The elasticity and strength of paper and other fibrous materials. British journal of applied physics. 1952;3:72.
[31] Zhang Z, Liu B, Huang Y, Hwang K, Gao H. Mechanical properties of unidirectional nanocomposites with non-uniformly or randomly staggered platelet distribution. Journal of the

Mechanics and Physics of Solids. 2010;58:1646-60.
[32] Szczesny SE, Elliott DM. Incorporating plasticity of the interfibrillar matrix in shear lag models is necessary to replicate the multiscale mechanics of tendon fascicles. Journal of the Mechanical Behavior of Biomedical Materials. 2014;40:325-38.
[33] Aspden R. Fibre reinforcing by collagen in cartilage and soft connective tissues. Proceedings of the Royal Society of London B: Biological Sciences. 1994;258:195-200.
[34] Gao H, Ji B, Jäger IL, Arzt E, Fratzl P. Materials become insensitive to flaws at nanoscale: lessons from nature. Proceedings of the National Academy of Sciences. 2003;100:5597-600.
[35] Goh KL, Meakin JR, Aspden RM, Hukins DW. Stress transfer in collagen fibrils reinforcing connective tissues: effects of collagen fibril slenderness and relative stiffness. Journal of theoretical biology. 2007;245:305-11.
[36] Szczesny SE, Elliott DM. Interfibrillar shear stress is the loading mechanism of collagen fibrils in tendon. Acta Biomaterialia. 2014;10:2582-90.
[37] Ahmadzadeh H, Connizzo BK, Freedman BR, Soslowsky LJ, Shenoy VB. Determining the contribution of glycosaminoglycans to tendon mechanical properties with a modified shear-lag model. Journal of biomechanics. 2013;46:2497-503.
[38] Slesarenko V, Volokh KY, Aboudi J, Rudykh S. Understanding the strength of bioinspired soft composites. International Journal of Mechanical Sciences. 2017;131:171-8.
[39] Singh A, Kallakuri S, Chen C, Cavanaugh JM. Structural and functional changes in nerve roots due to tension at various strains and strain rates: an in-vivo study. Journal of neurotrauma. 2009;26:627-40.
[40] Cloots RJ, van Dommelen JA, Kleiven S, Geers MG. Multi-scale mechanics of traumatic brain injury: predicting axonal strains from head loads. Biomechanics and modeling in mechanobiology. 2013:1-14.
[41] Wegmann S, Schöler J, Bippes CA, Mandelkow E, Muller DJ. Competing interactions stabilize pro-and anti-aggregant conformations of human tau. Journal of Biological Chemistry. 2011;286:20512-24.
[42] Ritchie RO. The conflicts between strength and toughness. Nature materials. 2011;10:817-22.
[43] Timoshenko S. Strength of Materials. Part I: Elementary Theory and Problems, 3rd edition. Malabar, Florida: Krieger Publishing Company, 1956.
[44] Janmey PA, Euteneuer U, Traub P, Schliwa M. Viscoelastic properties of vimentin compared with other filamentous biopolymer networks. The Journal of cell biology. 1991;113:155-60.
[45] Chełminiak P, Dixon J, Tuszyński J. Torsional elastic deformations of microtubules within continuous sheet model. The European Physical Journal E: Soft Matter and Biological Physics. 2010;31:215-27.
[46] Sarangapani KK, Akiyoshi B, Duggan NM, Biggins S, Asbury CL. Phosphoregulation promotes release of kinetochores from dynamic microtubules via multiple mechanisms. Proceedings of the National Academy of Sciences. 2013;110:7282-7.
[47] Spillantini MG, Goedert M. Tau protein pathology in neurodegenerative diseases. Trends in neurosciences. 1998;21:428-33.

[48] Hirokawa N, Shiomura Y, Okabe S. Tau proteins: the molecular structure and mode of binding on microtubules. The Journal of cell biology. 1988;107:1449-59.
[49] Soheilypour M, Peyro M, Peter SJ, Mofrad MR. Buckling behavior of individual and bundled microtubules. Biophysical journal. 2015;108:1718-26.
[50] Suresh S. Biomechanics and biophysics of cancer cells. Acta Materialia. 2007;55:3989-4014.
[51] Bell GI. Models for the specific adhesion of cells to cells. Science. 1978;200:618-27.
[52] Smith DH, Wolf JA, Lusardi TA, Lee VM-Y, Meaney DF. High tolerance and delayed elastic response of cultured axons to dynamic stretch injury. Journal of Neuroscience. 1999;19:4263-9.
[53] Yuen TJ, Browne KD, Iwata A, Smith DH. Sodium channelopathy induced by mild axonal trauma worsens outcome after a repeat injury. Journal of neuroscience research. 2009;87:3620-5.
[54] Chen B, Wu PD, Gao H. A characteristic length for stress transfer in the nanostructure of biological composites. Composites Science and Technology. 2009;69:1160-4.
[55] Wu J, Yuan H, Liu R. Theory and calculation of stress transfer between fiber and matrix. Applied Mathematics and Mechanics. 2015;36:815-26.
[56] Baas PW, Vidya Nadar C, Myers KA. Axonal Transport of Microtubules: the Long and Short of It. Traffic. 2006;7:490-8.
[57] Mehrbod M, Mofrad MR. On the significance of microtubule flexural behavior in cytoskeletal mechanics. PloS one. 2011;6:e25627.
[58] Dollé J-P, Morrison III B, Schloss RS, Yarmush ML. An organotypic uniaxial strain model using microfluidics. Lab on a Chip. 2013;13:432-42.
[59] Meaney D. Relationship between structural modeling and hyperelastic material behavior: application to CNS white matter. Biomechanics and modeling in mechanobiology. 2003;1:279-93.
[60] Drechsel DN, Hyman A, Cobb MH, Kirschner M. Modulation of the dynamic instability of tubulin assembly by the microtubule-associated protein tau. Molecular biology of the cell. 1992;3:1141-54.
[61] Bernal R, Pullarkat PA, Melo F. Mechanical properties of axons. Physical Review Letters. 2007;99:018301.
[62] Wright RM, Ramesh K. An axonal strain injury criterion for traumatic brain injury. Biomechanics and modeling in mechanobiology. 2012;11:245.
[63] Mac Donald C, Dikranian K, Song S, Bayly P, Holtzman D, Brody D. Detection of traumatic axonal injury with diffusion tensor imaging in a mouse model of traumatic brain injury. Experimental neurology. 2007;205:116-31.
[64] Bennett RE, Mac Donald CL, Brody DL. Diffusion tensor imaging detects axonal injury in a mouse model of repetitive closed-skull traumatic brain injury. Neuroscience letters. 2012;513:160-5.
[65] Wu J, Yuan H, Li L, Fan K, Qian S, Li B. Viscoelastic shear lag model to predict the micromechanical behavior of tendon under dynamic tensile loading. Journal of theoretical biology. 2018;437:202-13.
[66] Barthelat F, Dastjerdi AK, Rabiei R. An improved failure criterion for biological and engineered staggered composites. Journal of the Royal Society, Interface. 2013;10:20120849.
[67] Begley MR, Philips NR, Compton BG, Wilbrink DV, Ritchie RO, Utz M. Micromechanical models to guide the development of synthetic ‘brick and mortar’ composites. Journal of the Mechanics

and Physics of Solids. 2012;60:1545-60.
[68] Aumeier C, Schaedel L, Gaillard J, John K, Blanchoin L, Théry M. Self-repair promotes microtubule rescue. Nature cell biology. 2016.
[69] McKee AC, Cantu RC, Nowinski CJ, Hedley-Whyte ET, Gavett BE, Budson AE, et al. Chronic traumatic encephalopathy in athletes: progressive tauopathy after repetitive head injury. Journal of Neuropathology & Experimental Neurology. 2009;68:709-35.
[70] Goriely A, Geers MG, Holzapfel GA, Jayamohan J, Jérusalem A, Sivaloganathan S, et al. Mechanics of the brain: perspectives, challenges, and opportunities. Biomechanics and modeling in mechanobiology. 2015;14:931-65.